Molecular Medicine

RESEARCH ARTICLE

Open Access

Alteration in branching morphogenesis via YAP/TAZ in fibroblasts of fetal lungs in an LPS-induced inflammation model

Hung-Shuo Ko[1], Vincent Laiman[2,3], Po-Nien Tsao[4], Chung-Ming Chen[5,6] and Hsiao-Chi Chuang[7,8,9,10,11*]

Abstract

Background Chorioamnionitis is a common cause of preterm birth and leads to serious complications in newborns. The objective of this study was to investigate the role of the Hippo signaling pathway in lung branching morphogenesis under a lipopolysaccharide (LPS)-induced inflammation model.

Materials and methods IMR-90 cells and ex vivo fetal lungs were treated with 0, 10, 30, or 50 μg/ml LPS for 24 and 72 h. Supernatant levels of lactate dehydrogenase (LDH), interleukin (IL)-6, IL-8, Chemokine (C-X-C motif) ligand 1(CXCL1), branching and the surface area ratio, Yes-associated protein (YAP), transcription coactivator with PDZ-binding motif (TAZ), fibroblast growth factor 10 (FGF10), fibroblast growth factor receptor II (FGFR2), SRY-box transcription factor 2 (SOX2), SOX9, and sirtuin 1 (SIRT1) levels were examined. Differentially expressed genes in fetal lungs after LPS treatment were identified by RNA-sequencing.

Results LPS at 50 μg/ml increased IL-6 and IL-8 in IMR-90 cells and increased IL-6, CXCL1 and LDH in fetal lungs. The branching ratio significantly increased by LPS at 30 μg/ml compared to the control but the increased level had decreased by 50 μg/ml LPS exposure. Exposure to 50 μg/ml LPS increased phosphorylated (p)-YAP, p-YAP/YAP, and p-TAZ/TAZ in IMR-90 cells, whereas 50 μg/ml LPS decreased FGF10 and SOX2. Consistently, p-YAP/YAP and p-TAZ/TAZ were increased in fibronectin^{+} cells of fetal lungs. Moreover, results of RNA-sequencing in fetal lungs showed that SMAD, FGF, IκB phosphorylation, tissue remodeling and homeostasis was involved in branching morphogenesis following exposure to 50 μg/ml LPS. The p-SIRT1/SIRT1 ratio increased in IMR-90 cells by LPS treatment.

Conclusions This study showed that regulation of the Hippo pathway in fibroblasts of fetal lungs was involved in branching morphogenesis under an inflammatory disease such as chorioamnionitis.

Keywords Fibroblast, Hippo signaling pathway, Inflammation, Morphogenesis, Pseudoglandular stage

*Correspondence:
Hsiao-Chi Chuang
chuanghc@tmu.edu.tw
[1] School of Medicine, College of Medicine, Taipei Medical University, Taipei, Taiwan
[2] International Ph.D. Program in Medicine, College of Medicine, Taipei Medical University, Taipei, Taiwan
[3] Department of Anatomical Pathology, Faculty of Medicine, Public Health, and Nursing, Dr. Sardjito Hospital, Universitas Gadjah Mada, Yogyakarta, Indonesia
[4] Department of Pediatrics, National Taiwan University Hospital, Taipei, Taiwan
[5] Department of Pediatrics, Taipei Medical University Hospital, Taipei, Taiwan
[6] Department of Pediatrics, School of Medicine, College of Medicine, Taipei Medical University, Taipei, Taiwan
[7] School of Respiratory Therapy, College of Medicine, Taipei Medical University, 250 Wuxing Street, Taipei 11031, Taiwan
[8] Division of Pulmonary Medicine, Department of Internal Medicine, Shuang Ho Hospital, Taipei Medical University, New Taipei City, Taiwan
[9] Cell Physiology and Molecular Image Research Center, Wan Fang Hospital, Taipei Medical University, Taipei, Taiwan
[10] Graduate Institute of Medical Sciences, College of Medicine, Taipei Medical University, Taipei, Taiwan
[11] National Heart & Lung Institute, Imperial College London, London, UK

© The Author(s) 2023. **Open Access** This article is licensed under a Creative Commons Attribution 4.0 International License, which permits use, sharing, adaptation, distribution and reproduction in any medium or format, as long as you give appropriate credit to the original author(s) and the source, provide a link to the Creative Commons licence, and indicate if changes were made. The images or other third party material in this article are included in the article's Creative Commons licence, unless indicated otherwise in a credit line to the material. If material is not included in the article's Creative Commons licence and your intended use is not permitted by statutory regulation or exceeds the permitted use, you will need to obtain permission directly from the copyright holder. To view a copy of this licence, visit http://creativecommons.org/licenses/by/4.0/.

Introduction

Distributing the air to the gas-exchange zone of the lungs is achieved by the conducting airways in mature lungs. Formation of this tree-like system is mostly performed in the pseudoglandular stage which occurs from embryonic day 10.5 (E10.5) to E16.5 in mice and 6 to 16 weeks post-menstrual age (PMA) in humans (Smith et al. 2010). Two primary buds undergo a branching process to establish the airway structure, and nearly 20 generations of future airways are completed (Kitaoka et al. 1996). Impairment of branching morphogenesis was associated with lung hypoplasia which accounts for approximately 7–26% of neonatal autopsies (Husain and Hessel 1993), resulting in high rates of morbidity and mortality in newborns, such as congenital diaphragmatic hernias (Coughlin et al. 2016). Previous studies showed that lung branching was related to antenatal exposure to inflammatory mediators such as interleukin (IL)-6 and IL-8 (Dame and Juul 2000; Nogueira-Silva et al. 2006). Chorioamnionitis is defined as inflammation of the membrane and chorion of the placenta, which is known to be a frequent cause of preterm births (Tita and Andrews 2010). A dramatic increase in IL-6 in the amniotic fluid was observed in chorioamnionitis patients (Tsuda et al. 1998). However, the underlying mechanism regarding branching morphogenesis under chorioamnionitis is still unknown.

Chorioamnionitis, the most common type of antenatal inflammation, predominantly presents with intra-amniotic inflammation but with no evidence of microbial invasion (Kunzmann et al. 2013). Several risk factors were identified for chorioamnionitis, including bacterial vaginosis, group B streptococci, alcohol and tobacco use (Tita and Andrews 2010). Inflammatory mediators are first induced by a maternal immune response, followed by fetal inflammatory response syndrome, which causes the fetus to develop serious complications (Gomez et al. 1998; Higgins et al. 2016). A meta-analysis reported that chorioamnionitis was associated with a decreased risk of respiratory distress syndrome (RDS) and increased risk of bronchopulmonary dysplasia (BPD) (Sarno et al. 2021). Therefore, chorioamnionitis causes lung maturation and injury, and increases the risk of chronic lung diseases (CLDs) in preterm infants.

Fibroblasts are vital to the development of all stages of the lungs. Interactions between epithelial cells and fibroblasts rely on the proximity to the epithelium (Caniggia et al. 1991). During the pseudoglandular stage, fibroblasts stimulate cell proliferation in the lung epithelium, while promoting cell differentiation in the saccular stage (Caniggia et al. 1992). The formation and remodeling of the extracellular matrix (ECM) via matrix-fibroblasts, lipofibroblasts, and myofibroblasts in the process of lung development create tensile strength (Ushakumary et al. 2021). Lipofibroblasts are capable of taking up triglycerides, which support the synthesis of surfactants in type 2 alveolar epithelial cells (Torday and Rehan 2016), and they were also demonstrated to protect the lungs from hyperoxic injury (Rehan et al. 2006). Myofibroblasts play a key role in alveologenesis through activating platelet-derived growth factor (PDGF)/PDGF receptor (PDGFR)-α signaling, which was validated by inactivating the pathway which suspended alveolarization in mice (Boström et al. 2002; Boström et al. 1996). Recently, alveolar niche cells were categorized as fibroblasts and were observed to support alveolar epithelial regeneration after injury (Zepp et al. 2017).

The Hippo signaling pathway is considered to be crucial for lung development (Fu et al. 2017). The Yes-associated protein (YAP) and transcriptional coactivator with PDZ-binding motif (TAZ) are key downstream components of the Hippo signaling kinase pathway. Isago and colleagues reported that YAP-conditioned knockout in mice caused blockade of branching morphogenesis, whereas a TAZ deficiency gave rise to an emphysema-like phenotype in adult mice (Isago et al. 2020). They also showed that sonic hedgehog, which inhibits the expression of fibroblast growth factor 10 (FGF10) in the mesenchyme, is upregulated by YAP and TAZ in the lung epithelium. FGF10 is considered to be an essential protein in the early stage of lung development (Bellusci et al. 1997). Localized dynamic expression of FGF10 in the mesenchyme adjacent to the distal bud plays an important role in directing outgrowth (Bellusci et al. 1997). Activation of cytoplasmic YAP inhibited FGF10 expression to ensure lung epithelial lineage commitment (Volckaert et al. 2019). Suppression of FGF10 resulted in non-branching trachea (Sekine et al. 1999); in contrast, overexpression of FGF10 brought about aberrant bronchial growth (Isago et al. 2020). Furthermore, the boundary between the airway and distal lung was marked through a nucleocytoplasmic shift of YAP, and it was observed that a YAP deficiency led to SRY-box transcription 9 $(SOX9)^{pos}$ domain expansion and failure to form tube-like airway structures (Mahoney et al. 2014). Those studies suggested that YAP/TAZ play important roles in lung morphogenesis; however, the role of YAP/TAZ in regulating fibroblasts in antenatal inflammation remains unclear. The objective of this study was to investigate regulation of the Hippo signaling pathway in fibroblasts of fetal lungs in a lipopolysaccharide (LPS)-induced inflammation model.

Materials and methods

Cell culture and treatment

Human fetal lung IMR-90 fibroblast cells (derived from a 16-week-old female Caucasian fetus) were obtained from the Bioresource Collection and Research Center

(Hsinchu, Taiwan). Cells were cultured in 90% minimum essential medium (MEM) with 2 mM L-glutamine and Earle's balanced salt solution (BSS) adjusted to contain 1.5 g/l sodium bicarbonate, 0.1 mM non-essential amino acids, 1.0 mM sodium pyruvate (Corning, Corning, NY, USA), and 10% fetal bovine serum (FBS) under 5% CO_2 and 95% relative humidity at 37 °C. Cells were exposed to 10, 30, and 50 μg/ml LPS (*Escherichia coli* O111:B4, Sigma-Aldrich, St. Louis, MO, USA) and control medium (0 μg/ml) for 24 h.

Fetal lung ex vivo culture and treatment

Pregnant ICR mice were obtained from BioLASCO Taiwan (Taipei, Taiwan) and euthanized at E11.5 (at the pseudoglandular stage). Embryos was collected from the mice followed by lung dissection under a dissecting microscope. All lungs were cultured on Transwell® membranes (Corning) with Biggers, Gwatkin, and Judah (BGJb) medium (Gibco, Grand Island, NY, USA) containing 0.1% FBS, L-ascorbic acid, and primocin (InvivoGen, San Diego, CA, USA). Fetal lungs were exposed to 0, 10, 30, and 50 μg/ml LPS under 5% CO_2 and 95% relative humidity at 37 °C for 3 days. Medium was collected and replaced everyday. The lung morphology was investigated every 24 h using a Leadview 2000AIO Digital Camera (Taipei, Taiwan). The surface area of the fetal lungs and the number of buds were calculated by ImageJ software (vers. 1.53, National Institutes of Health (NIH), Bethesda, MD, USA) after being normalized to the first day of the experiment.

Lactate dehydrogenase (LDH)

Supernatants were collected from cells and fetal lung ex vivo culture for an LDH cytotoxicity assay (Donjido Molecular Technology, Rockville, MD, USA). Details of the experimental procedures were in accordance with the manufacturer's instructions.

Enzyme-linked immunosorbent assay

IL-6, IL-8 and chemokine (C-X-C motif) ligand 1(CXCL1) levels in supernatants collected from cells and fetal lung culture were examined using enzyme-linked immunosorbent assay (ELISA) kits (ThermoFisher Scientific, Waltham, MA, USA and R&D Systems, Minneapolis, MN, USA). Details of the experimental procedures were in accordance with the manufacturer's instructions.

Western blot analysis

Protein from cells and fetal lungs was collected with lysis buffer (Sigma-Aldrich, St. Louis, MO, USA). Samples were electrophoresed in 10% sodium dodecylsulfate polyacrylamide gel electrophoresis (SDS-PAGE) gels and transferred to polyvinylidene difluoride (PVDF) membranes. Membranes were blocked with non-fat dried milk diluted in Tris-buffered saline/Tween-20 (TBST) for 1 h. Samples were incubated with primary antibodies including mouse anti-YAP (1:1000; Proteintech, Rosemont, IL, USA), rabbit anti-p-YAP (1:1000; Abcam, Cambridge, UK), rabbit anti-TAZ (1:1000; Cell Signaling, Danvers, MA, USA), rabbit anti-p-TAZ (1:1000; Cell signaling), rabbit anti-FGF10 (1:1000; Abcam), rabbit anti-FGFR2 (1:1000; Abcam), rabbit anti-SOX2 (1:1000; Cell Signaling), rabbit anti-SOX9 (1:1000; Cell Signaling), rabbit anti-SIRT1 (1:1000; Cell Signaling), rabbit anti p-SIRT1 (1:1000; Signalway Antibody, Greenbelt, MD, USA), and mouse anti-β-actin (1:5000; Proteintech) overnight at 4 °C. After incubation with secondary antibodies for 1 h at room temperature, protein bands were detected with the ChemiDoc™ MP Imaging system (Bio-Rad, Hercules, CA, USA) and quantified by Image-Pro software (vers. 4, Media Cybernetics, Rockville, MD, USA). All data were normalized to the control.

Immunofluorescence (IF)

Paraffin-embedded fetal lung tissue sections were placed in an oven at 60 °C and rehydrated before staining. Antigen retrieval was done by undergoing heating with citrate buffer (pH 6.0). Bovine serum albumin (BSA, Bionova Scientific, Fremont, CA, USA) with 0.25% Triton X-100 was used for cell permeabilization and 5% BSA was used for blocking at room temperature, followed by incubation with a primary antibody, mouse conjugated fibronectin (1:250; Santa Cruz Biotechnology, Dallas, Tx, USA) for 1.5 h and another primary unconjugated antibody consisting of mouse anti-YAP (1:400; Proteintech), rabbit anti-p-YAP (1:400; Abcam), rabbit anti-TAZ (1:500; Cell Signaling), rabbit anti-p-TAZ (1:500; Cell Signaling), rabbit anti-FGF10 (1:250; BOSTER BIO, Pleasanton, CA, USA), rabbit anti-SOX2 (1:400; Cell Signaling), rabbit anti-SOX9 (1:200; ABGENT, San Diego, CA, USA), rabbit anti-SIRT1 (1:400; Cell Signaling), and rabbit anti p-SIRT1 (1:200; Cell Signaling). A fluorophore-conjugated secondary antibody against the primary antibody was used, and then the sample was covered with mounting medium containing 4′,6-diamidino-2-phenylindole (DAPI, Abcam). Samples were imaged by confocal fluorescence microscopy (TCS SP5, Leica, Wetzlar, Germany) equipped with a camera and imaging software (SPOT Imaging, Sterling-Heights, MI, USA) at 400× magnification. The co-expression mean intensities of YAP, p-YAP, TAZ, p-TAZ, FGF10, SOX2, SOX9, SIRT1, and p-SIRT1 that were fibronectin positive (fibronectin$^+$; for identifying fibroblasts) in five different regions were quantified by ImageJ software (NIH) as previously reported (Shihan et al. 2021).

Immunocytochemistry (ICC)

IMR-90 cells were cultured and then fixed by 2% formaldehyde in PBS for 15 min at room temperature before staining. 0.5% Triton X-100 was used for permeabilization and 5% BSA in PBS was used for blocking at room temperature, followed by incubation with a primary antibody including mouse anti-YAP (1:400; Proteintech), rabbit anti-p-YAP (1:400; Affinity, Melbourne, Victoria, Australia), rabbit anti-TAZ (1:400; Cell Signaling) and rabbit anti-p-TAZ (1:400; Cell Signaling) overnight at 4 °C. A fluorophore-conjugated secondary antibody against the primary antibody was used, and then the sample was covered with mounting medium containing DAPI. Samples were imaged by confocal fluorescence microscopy equipped with a camera and imaging software as the above mentioned at 200× magnification.

RNA-sequencing

Total RNA was collected from fetal lung tissues in Trizol® reagent (Ambion, Life Technologies, Carlsbad, NY, USA) after exposure to 50 μg/ml LPS and control medium. The purity and quantification were checked using a SimpliNano™-Biochrom Spectrophotometer (Biochrom, Holliston, MA, USA). A Qsep 100 DNA/RNA Analyzer (BiOptic, New Taipei, Taiwan) was used to monitor RNA degradation and integrity. Sequencing libraries were generated using a KAPA messenger (m)RNA HyperPrep Kit (KAPA Biosystems, Roche, Basel, Switzerland) following the manufacturer's instructions. The original data were obtained through the Illumina NOVAseq 6000 platform. Clean data were obtained by evaluating the parameters including low-quality reads, adaptor contamination, and base qualities. A gene ontology (GO) pathway enrichment analysis of differentially expressed genes (DEGs) was performed using clusterProfiler (vers. 4.4.0). A gene set enrichment analysis (GSEA) was used to identify enriched biological functions and activated pathways from a molecular signature database (MSigDB). A dotplot was created by Rstudio 10.14.

Statistical analysis

All data are expressed as the mean ± standard deviation (SD). Continuous variables were examined by a one-way analysis of variance (ANOVA) with Tukey's post-hoc or an unpaired *t*-test. Statistical analyses were performed using GraphPad Prism 7 (San Diego, CA, USA). A p value of < 0.05 was considered statistically significant.

Results

Cytotoxicity and inflammation

Inflammation and cytotoxicity in IMR-90 cells and fetal lung ex vivo culture were shown in Fig. 1. We observed that IL-6 was significantly increased by LPS compared to the control group in IMR-90 cells ($n=6$, $p<0.05$; Fig. 1A). IL-8 was significantly increased by 50 μg/ml LPS in IMR-90 ($n=3$, $p<0.05$; Fig. 1A). Consistently, IL-6 was increased by 50 μg/ml LPS during the 3 days of exposure in fetal lungs ($p<0.05$; Fig. 1B). CXCL1 was significantly increased by 30 and 50 μg/ml LPS in fetal lungs ($n=3$, $p<0.05$; Fig. 1B). We found that LDH was significantly increased by 50 μg/ml LPS on day 3 after exposure in fetal lungs ($n=6$, $p<0.05$; Fig. 1B). We also observed increasing enrichment scores for chemokine activity and genes including CXCL5, CCL7, CCL11, CXCL3, CXCL13, PF4, GRAMD2, CXCL10, CXCL2, CXCL1, CCL2 ($p<0.05$; Fig. 1C).

Lung branching morphogenesis

Figure 2 shows the effect of LPS on lung branching morphogenesis in fetal lungs. We observed that lung branching had significantly increased by day 3 after 30 μg/ml LPS exposure ($n=6$, $p<0.05$), but the increased level had decreased by day 3 after 50 μg/ml LPS exposure ($n=6$, $p<0.05$, Fig. 2A). We also observed increasing enrichment scores for lung epithelial cell proliferation and lung morphogenesis at 50 μg/ml LPS compared to the control ($p<0.05$, Fig. 2B).

YAP and TAZ phosphorylation in fibroblasts

Figure 3 shows YAP and TAZ expressions in fibroblasts in vitro and ex vivo fetal lungs after LPS treatment. We observed that p-YAP and p-YAP/YAP ratios had significantly increased by LPS at 50 μg/ml, and the p-TAZ/TAZ ratios had significantly increased by LPS at 30 and 50 μg/ml compared to the control group in IMR-90 cells (n = 6, $p<0.05$, Fig. 3A). We further observed decreased YAP and TAZ nuclear expressions with increased p-YAP and p-TAZ cytoplasm expressions after LPS at 30 and 50 μg/ml on IMR-90 cells (Additional file 1: Fig. S1). However, there was no significant difference in YAP or TAZ phosphorylation levels by LPS exposure in ex vivo fetal lungs (Fig. 3B). We next observed increased both fibronectin$^+$ p-YAP/YAP and pTAZ/TAZ ratio in fetal lungs at 50 μg/ml LPS, which is consistent with our results in IMR-90 cells (n = 3, $p<0.05$, Fig. 3C).

FGF10, SOX2, and SOX9 expressions by fibroblasts

Figure 4 shows FGF10, FGFR2, SOX2, and SOX9 expressions by fibroblasts in vitro and ex vivo after LPS treatment. We observed that FGF10 significantly decreased by LPS at 50 μg/ml, and SOX9 significantly decreased by LPS at 30 μg/ml compared to the control group. In addition, SOX2 significantly decreased by LPS at 30 and 50 μg/ml in IMR-90 cells ($n=6$, $p<0.05$, Fig. 4A). We observed that SOX9 significantly increased by LPS at 10 μg/ml with 3 days of exposure in fetal lungs ($n=6$,

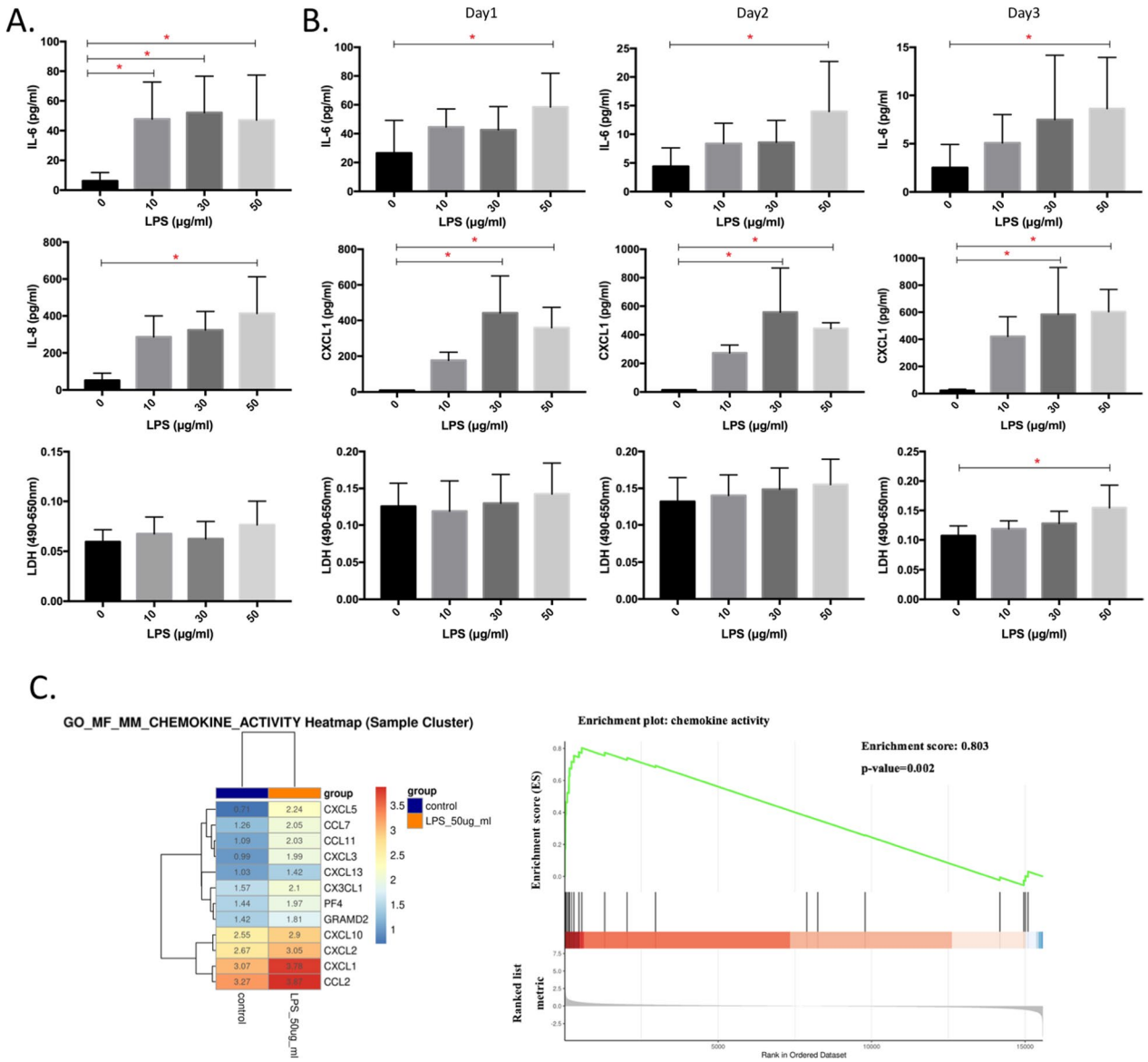

Fig. 1 Cytotoxicity and inflammation by lipopolysaccharide (LPS) in IMR-90 cells and ex vivo fetal lungs. **A** Interleukin (IL)-6 (n = 6), IL-8 (n = 3) and lactate dehydrogenase (LDH) (n = 6) in IMR-90 cell supernatants by LPS at 0 (control), 10, 30, and 50 μg/ml. **B** IL-6 (n = 6), CXCL1 (n = 3) and LDH (n = 6) in fetal lung supernatants by LPS at 0, 10, 30, and 50 μg/ml on days 1, 2 and 3. **C** Hierarchical clustering heatmap of significantly expressed gene and gene set enrichment analysis (GSEA) associated with cytokine activity in ex vivo fetal lungs treated by LPS at 0 and 50 μg/ml for 3 days. The activation Z-scores was displayed by the depth of the color (red: upregulation; blue: downregulation). *$p < 0.05$

$p < 0.05$, Fig. 4B). We further examined these protein expressions in fibroblasts with fibronectin$^+$ in fetal lungs; however, no significant differences were observed (Fig. 4C).

SIRT1 phosphorylation in fibroblasts

Figure 5 shows SIRT1 expression by fibroblasts in vitro and ex vivo after LPS treatment. We observed that the p-SIRT1/SIRT1 ratio significantly increased by LPS at 50 μg/ml compared to the control group in IMR-90 cells ($p < 0.05$, Fig. 5A). However, there was no significant difference in SIRT1 phosphorylation levels by LPS exposure in ex vivo fetal lungs (Fig. 5B). We further examined SIRT1 and p-SIRT1 expressions by fibroblasts with fibronectin$^+$ in fetal lungs; however, no significant difference was observed (Fig. 5C).

Molecular functions and biological pathways of fetal lung

Figure 6 shows molecular functions and biological pathways of fetal lungs after 3 days of LPS exposure.

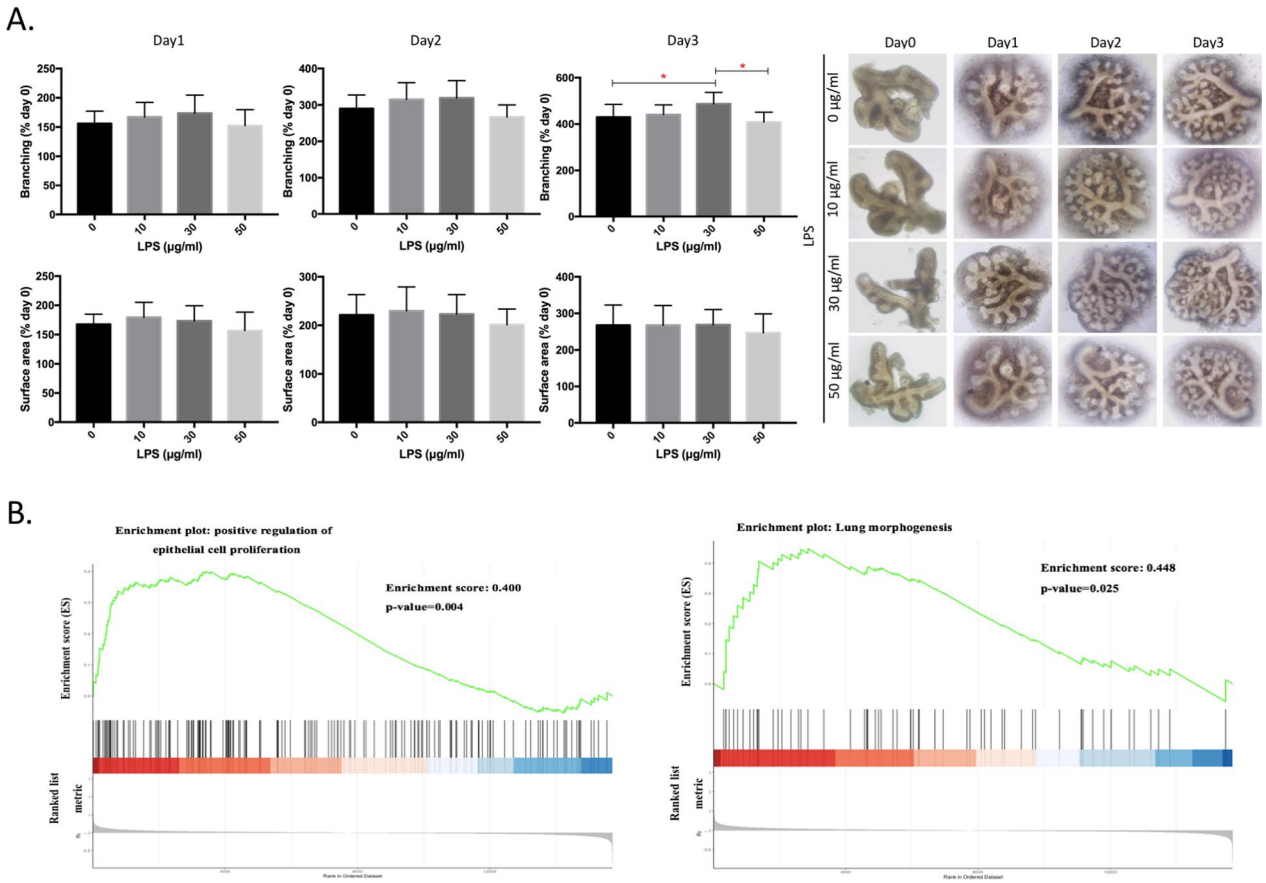

Fig. 2 Branching morphogenesis in ex vivo fetal lungs by lipopolysaccharide (LPS). **A** Branching and surface area ratios normalized to day 0 after LPS administration at 0, 10, 30, and 50 μg/ml on days 1, 2, and 3 ($n=6$). **B** GSEA of enrichment scores by LPS at 0 and 50 μg/ml for 3 days. *$p<0.05$

As to molecular functions, we observed upregulation of SMAD, (R)-SMAD, core promoter, activating transcription factor, growth factor, and fibroblast growth factor binding, as well as downregulation of proteoglycan binding, oxidoreductase acting on NADPH, NADH dehydrogenase, endopeptidase, and cysteine-type peptidase activity by LPS ($p<0.05$, Fig. 6A). In addition, we also observed both up- and downregulation of ECM binding by LPS ($p<0.05$, Fig. 6A). As to biological pathways, upregulation of spongiotrophoblast layer development, ribosomal small subunit assembly, response to stilbenoid, gene expression by genetic printing, IκB phosphorylation, formation of a translation preinitiation complex, dosage compensation, and cytoplasmic translation initiation as well as downregulation of tissue homeostasis and remodeling, bone resorption and remodeling, anatomical structure homeostasis, leukocyte proliferation, and defense of gram-negative bacterium were observed by LPS ($p<0.05$, Fig. 6B).

Discussion

The novelty of this study is that we investigated regulation of the Hippo signaling pathway in fibroblasts of fetal lungs in an LPS-induced inflammation model. The significances of our results are as follows: (1) LPS increased inflammation and cytotoxicity, leading to alterations in lung branching morphogenesis, (2) YAP and TAZ phosphorylation in fibroblasts of fetal lungs was activated by LPS, (3) FGF10, SOX2, and SOX9 were downregulated in fibroblasts of fetal lungs by LPS, and (4) SIRT1 phosphorylation in fibroblasts of fetal lungs was upregulated by LPS.

Proinflammatory cytokines of antenatal inflammation are associated with preterm labor (Murthy and Kennea 2007). Increasing evidence indicated that antenatal inflammation causes a systemic inflammatory response, leading to tissue injury in the newborn (Murthy and Kennea 2007). Clinical observations suggested that fetal inflammation increased the risk of BPD (Sarno

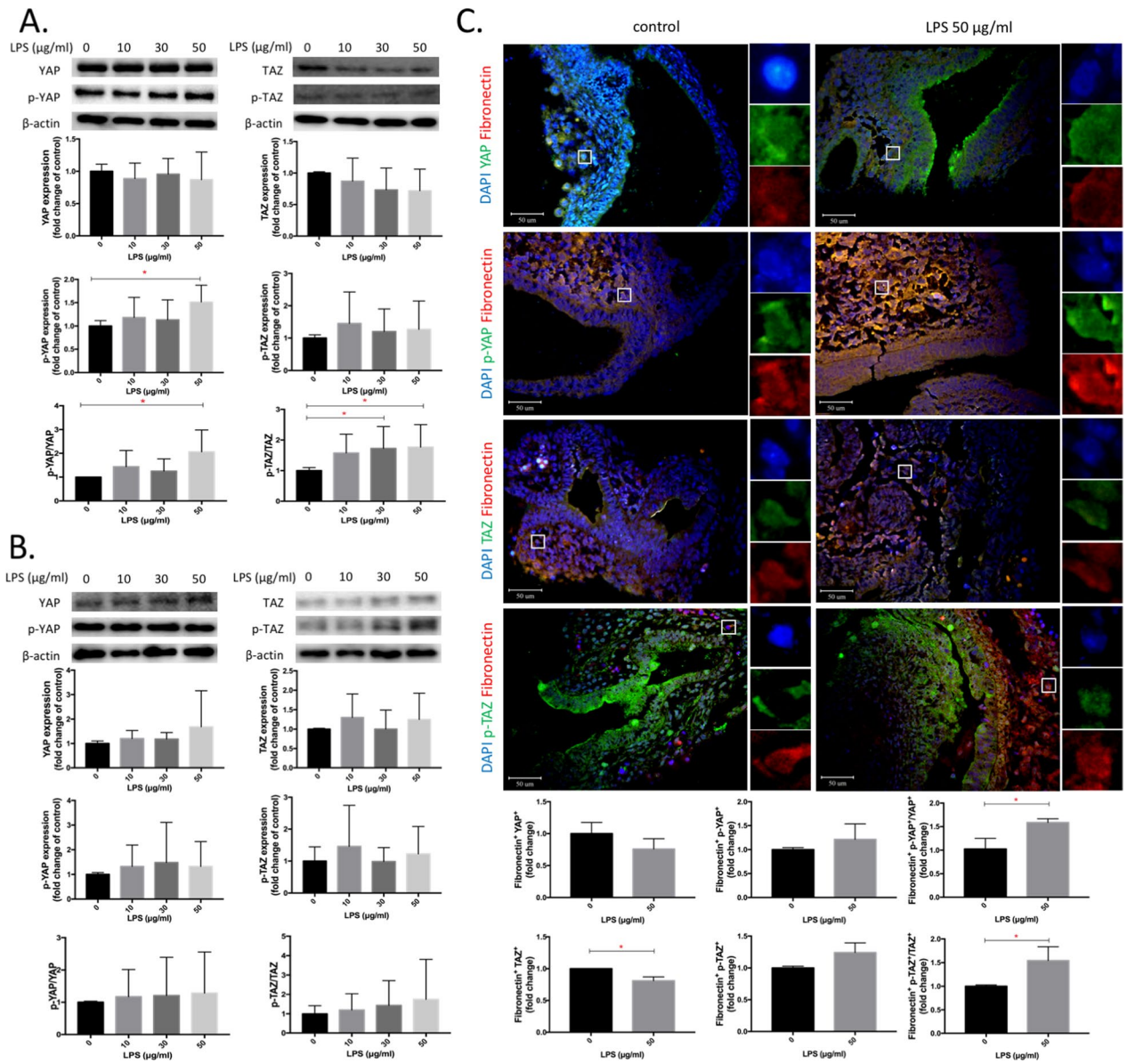

Fig. 3 Expression of Yes-associated protein (YAP), phosphorylated (p)-YAP, transcription coactivator with PD2-binding motif (TAZ) and p-TAZ in IMR-90 cells, ex vivo fetal lungs, and fibroblasts of ex vivo fetal lungs by lipopolysaccharide (LPS). **A** Expressions of YAP, p-YAP, p-YAP/YAP, TAZ, p-TAZ, and p-TAZ/TAZ in IMR-90 cells by LPS at 0, 10, 30, and 50 μg/ml for 24 h ($n=6$). **B** Expressions of YAP, p-YAP, p-YAP/YAP, TAZ, p-TAZ, and p-TAZ/TAZ in whole fetal lungs by LPS at 0, 10, 30, and 50 μg/ml for 3 days ($n=6$). **C** Expressions of fibronectin$^+$ YAP, p-YAP, p-YAP/YAP, TAZ, p-TAZ, and p-TAZ/TAZ of fetal lungs by LPS at 0 and 50 μg/ml for 3 days. DAPI (in blue) marked nuclear staining. Fibronectin (in red). YAP, p-YAP, TAZ, and p-TAZ (in green) ($n=3$). *$p<0.05$

et al. 2021). In our study, LPS was used to induce antenatal inflammation by increasing IL-6, IL-8 and CXCL1 in vitro and ex vivo. LPS has also been used to induce inflammation in lung epithelial cells (Kim et al. 2012; Hu et al. 2016). A previous study demonstrated that maternal exposure to LPS postponed the alveolarization of the lungs in rats (Cao et al. 2009). Another study reported that chicken embryos in the pseudoglandular stage persistently exposed to LPS exhibited restricted branching morphogenesis of the lungs (Long et al. 2018). Whole mouse fetal lung explants exposed to LPS in the pseudoglandular stage also showed similar results in a dose-dependent manner (Arai et al. 2020). Land and Darakhshan (2004) observed that LPS evoked spontaneous airway branching within a permissive concentration range in the pseudoglandular stage of fetal rat lungs.

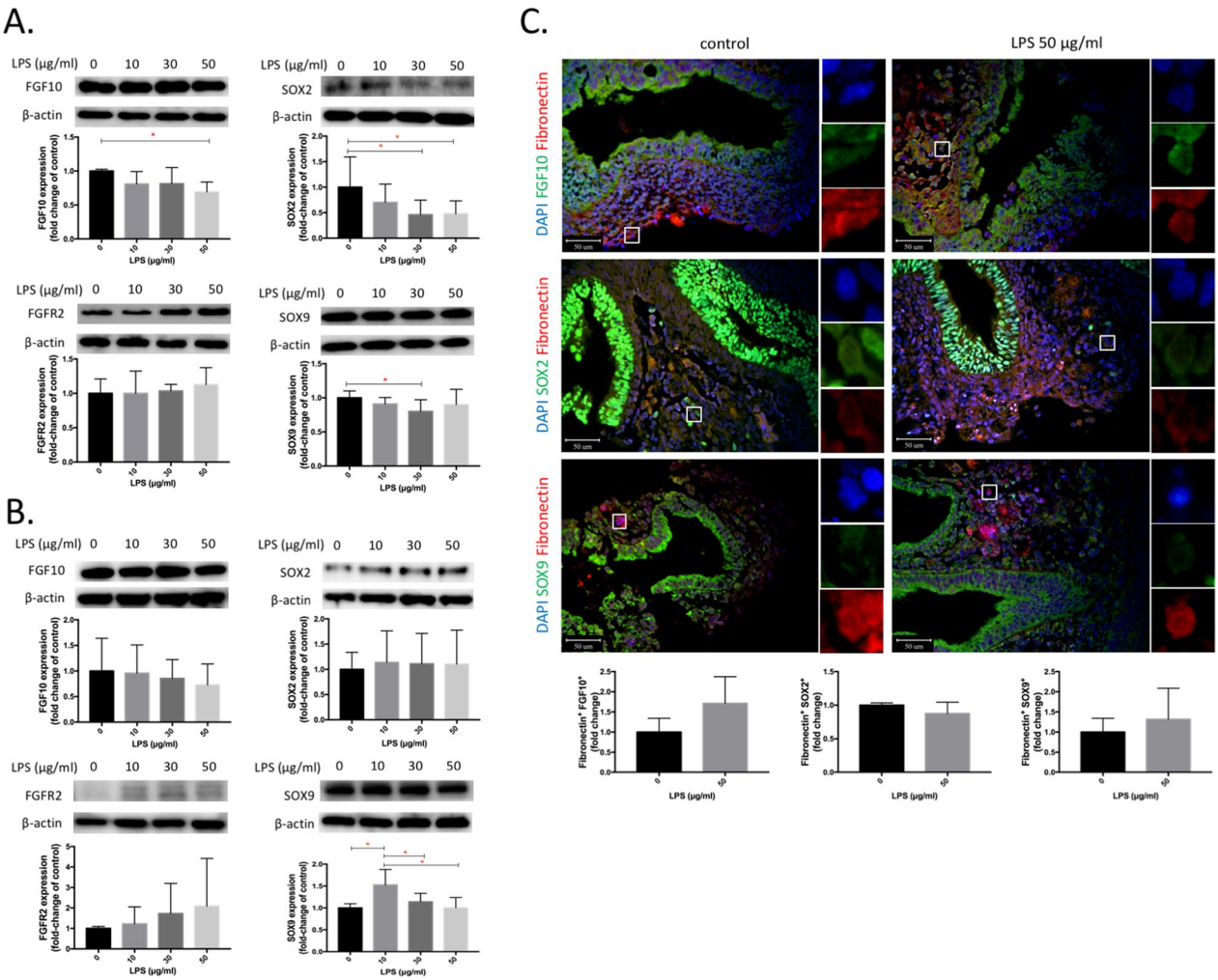

Fig. 4 Expressions of fibroblast growth factor 10 (FGF10), FGF receptor 2 (FGFR2), SRY-box transcription factor 2 (SOX2), and SOX9 in IMR-90 cells, ex vivo fetal lungs, and fibroblasts of ex vivo fetal lungs by lipopolysaccharide (LPS). **A** Expressions of FGF10, FGFR2, SOX2, and SOX9 in IMR-90 cells by LPS at 0, 10, 30, and 50 μg/ml for 24 h ($n=6$). **B** Expressions of FGF10, FGFR2, SOX2, and SOX9 in whole fetal lungs by LPS at 0, 10, 30, and 50 μg/ml for 3 days ($n=6$). **C** Expressions of fibronectin^{+} FGF10, SOX2, and SOX9 of fetal lungs by LPS at 0 and 50 μg/ml for 3 days. DAPI (in blue). Fibronectin (in red). FGF10, SOX2, and SOX9 (in green) ($n=3$). *$p<0.05$

In our study, we also observed the same phenomenon that the branching ratio increased at low concentrations of LPS, while the increasing level was significantly decreased by a high LPS concentration. Therefore, the results suggested that antenatal inflammation altered lung branching morphogenesis, which could rely on the severity of the inflammatory response.

We observed that LPS increased YAP and TAZ phosphorylation in fibroblasts of fetal lungs. YAP and TAZ are the main downstream mediators of the Hippo pathway, interact with TEA domain (TEAD) family members and activate cell proliferation when translocated into the nucleus, while inducing apoptosis when localized in the cytoplasm (Wang et al. 2017; Lin et al. 2015; Hansen et al. 2015). YAP and TAZ were previously reported to be required during embryonic development to undergo high rates of proliferation (Pocaterra et al. 2020). Previous studies demonstrated that YAP deficiency caused abnormal bronchial morphogenesis, leading to cyst-like structure with thin wall and decreased type 1 alveolar epithelial cells (Mahoney et al. 2014; Nantie et al. 2018; Lin et al. 2017). TAZ deficiency also resulted in emphysema-like changes in lung (Makita et al. 2008; Mitani et al. 2009). Additionally, YAP inhibitor was also reported to delay cell proliferation, epithelial regeneration and recovery of lung injury from LPS (Liu et al. 2020). The impaired regeneration of alveolar epithelial due to lack of YAP/TAZ was paralleled with NF-κB proinflammatory

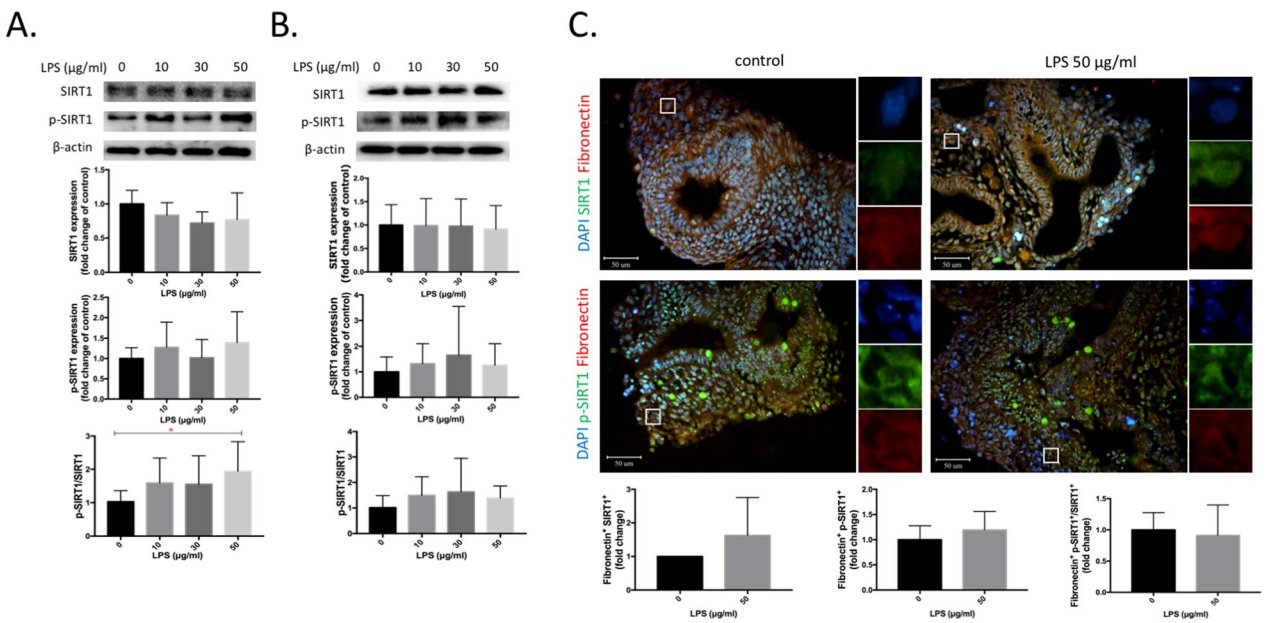

Fig. 5 Expressions of sirtuin 1 (SIRT1) and phosphorylated (p)-SIRT1 in IMR-90 cells, ex vivo fetal lungs, and fibroblasts of ex vivo fetal lungs by lipopolysaccharide (LPS). **A** Expressions of SIRT1, p-SIRT1, and p-SIRT1/SIRT1 in IMR-90 cells by LPS at 0, 10, 30, and 50 μg/ml for 24 h ($n=6$). **B** Expressions of SIRT1, p-SIRT1, and p-SIRT1/SIRT1 in whole fetal lungs by LPS at 0, 10, 30, and 50 μg/ml for 3 days ($n=6$). **C** Expressions of fibronectin$^+$ SIRT1, p-SIRT1, and p-SIRT1/SIRT1 of fetal lungs by LPS at 0 and 50 μg/ml for 3 days. DAPI (in blue). Fibronectin (in red). SIRT1, p-SIRT1 (in green) ($n=3$). *$p<0.05$

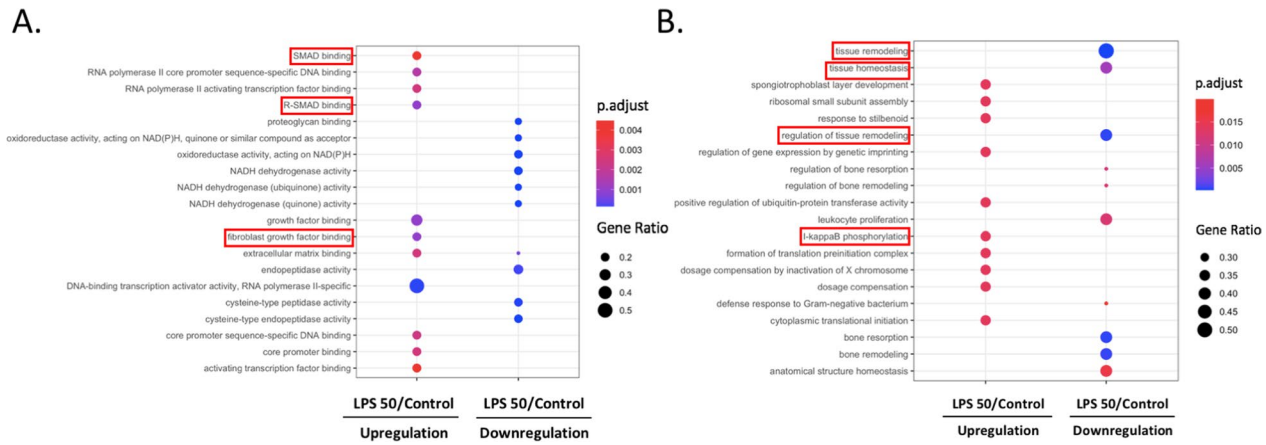

Fig. 6 RNA sequencing of ex vivo fetal lungs treated with lipopolysaccharide (LPS). **A** Gene ontology (GO) analysis of molecular functions of genes by LPS at 0 and 50 μg/ml for 3 days. **B** GO analysis of biologic pathways of genes by LPS at 0 and 50 μg/ml for 3 days

signal pathway, which inhibited lung branching and epithelial growth (LaCanna et al. 2019; Muraoka et al. 2000). Lung branching morphogenesis requires epithelial-mesenchymal interactions (Hogan and Yingling 1998). It was proven that two primary lung buds without mesenchyme stops processing branching (Wessells 1970). Our findings suggest that regulation of the Hippo pathway in the surrounding mesenchyme, such as fibroblasts, occurred by LPS in fetal lungs. Together, this suggested that the phosphorylation of YAP and TAZ in fibroblasts by LPS could be relevant to abnormal branching under inflammation.

Next, we observed decreased expressions of FGF10, SOX2, and SOX9 in fibroblasts after LPS treatment. FGF10 is secreted by fibroblasts of the mesenchyme and guides lung epithelial branching (Yin and Ornitz 2020). A previous study showed that lung hypoplasia with esophageal atresia was caused by downregulating FGF10

signaling in vivo (Wang et al. 2018a). Another study reported that LPS affected branching morphogenesis via decreasing *FGF10* gene expression (Muratore et al. 2009). Consistent with our results, high dose LPS significant reduced FGF10 expression and might be negatively associated with lung branching morphogenesis (Benjamin et al. 2010). SOX2 and SOX9 play essential roles in the proliferation and differentiation of the proximal and distal lung epithelium, respectively (Danopoulos et al. 2018). SOX2 is restricted to the proximal lung epithelium during lung development (Gontan et al. 2008). A previous study demonstrated that the loss of SOX2 led to an immature secretory and ciliated system in conducting airways (Tompkins et al. 2011). SOX9 is expressed by the distal lung epithelium as well as in the mesenchyme surrounding the proximal lung (Fernandes-Silva et al. 2017). It was found to promote branching morphogenesis by regulating not merely the balance between distal epithelium differentiation and proliferation but the ECM as well (Rockich et al. 2013). As a consequence, decreasing expressions of FGF10, SOX2 and SOX9 by fibroblasts with LPS treatment could be associated with branching defects under inflammation (Mia and Singh 2022).

SIRT1, a NAD^+-dependent deacetylase, is an anti-apoptotic factor and increases resistance to oxidative damage in mammalian cells (Alcendor et al. 2007). In our study, we found increased SIRT1 phosphorylation in fibroblasts of fetal lungs after LPS treatment. Previous study showed that SIRT1 phosphorylation by administration of dexmedetomidine significantly reduce sepsis-induced lung injury in rat model (Wang et al. 2020). Another study showed that SIRT1 phosphorylation was associated with anti-oxidative and anti-inflammation on endothelial cells (Kitada et al. 2016). SIRT1 phosphorylation can attenuate drug induced apoptosis and coactivated heat shock factor 1, which was responsible for activate the protective factors in response to stress (Wang et al. 2018b; Monteiro and Cano 2011). Consistently, SIRT1 overexpression protected normal human fibroblast IMR-90 cells from H_2O_2 injury, with loss of SIRT1 phosphorylation resulted in decreased activity and loss of survivability (Luo et al. 2001; Sasaki et al. 2008). SIRT1 was also found to alleviate LPS-induced lung injury in animal models by decreasing the endothelial permeability (Fu et al. 2019). Taken together, SIRT1 phosphorylation in fibroblasts under LPS-induced inflammation might be associated with a protective mechanism to mitigate injury from inflammation.

Based on RNA-sequencing results, we observed that LPS exposure upregulated the binding ability including SMAD and FGF. The *SMAD* gene is involved in the TGF-β and BMP signaling pathway (Zhao et al. 1998). SMAD-2, -3, and -7 are responsible for *TFG-β* gene expression, and several studies demonstrated that the addition of exogenous TGF-β inhibited lung branching (Warburton et al. 2003). A BMP-specific receptor regulates Smads (R-Smads) including SMAD-1, -5, and -8 and transduces the BMP4 ligand into nuclei (Massagué and Chen 2000). Overexpression of BMP4 promoted by the SP-C enhancer caused abnormalities in the lungs with cystic terminal sacs and inhibition of epithelial cell proliferation (Bellusci et al. 1996). Similar results were also observed in localized FGF10 overexpression in fetal rat lungs (Gonzaga et al. 2008). In addition, we also observed that LPS upregulated the phosphorylation of IκB. Phosphorylation of IκB activates nuclear factor (NF)-κB, which is regarded as a proinflammatory signal pathway (Karin and Ben-Neriah 2000; Lawrence 2009). A previous study found that activation of NF-κB in the mesenchyme inhibited lung branching and epithelial growth (Muraoka et al. 2000). Consistently, the downregulation of tissue homeostasis and remodelling by LPS were observed. Hippo signaling pathway was previously reported to be involved in tissue homeostasis and remodeling, with delayed cell proliferation, epithelial regeneration and lung injury recovery from LPS by YAP inhibitor (Liu et al. 2020; Mia and Singh 2022). The impaired regeneration of alveolar epithelial due to lack of YAP/TAZ was accompanied with failure in terminating NF-κB proinflammatory signal pathway (LaCanna et al. 2019). Taken together, abnormal branching was confirmed by the results from RNA-sequencing under LPS-induced inflammation in fetal lungs.

These are the first data to our knowledge showing dysregulation of the Hippo signaling pathway in fibroblasts of fetal lungs in an LPS-induced inflammation model, as depicted in a summary schematic (Fig. 7). There are some limitations to our study. Future studies should be conducted to clarify the biphasic model of branching morphogenesis in different developing stages of the lungs, confirm the senescence and the relationship between phosphorylation of SIRT1 and its activity in our study. In addition, future study by performing block and rescue method will be performed to confirm YAP/TAZ regulated lung branching.

Conclusions

In conclusion, our results suggested that abnormal branching occurred under LPS-induced inflammation, which involved regulation of the Hippo pathway via YAP/TAZ phosphorylation in fibroblasts of fetal lungs. This study showed the importance of understanding the role of the Hippo pathway in the surrounding mesenchyme of fetal lungs under inflammation. Clinically, it could help us understand the relationship between antenatal inflammation and lung branching.

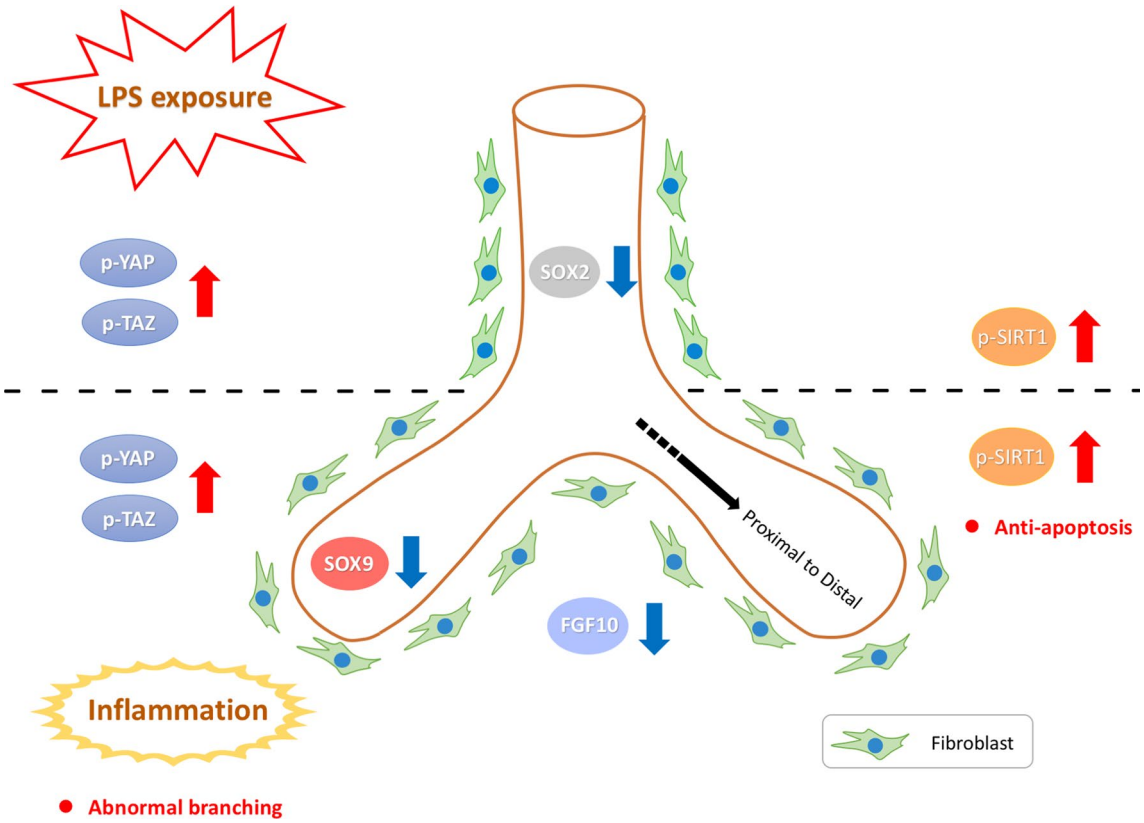

Fig. 7 Summary. High dose LPS exposure induced the inflammatory response and led to YAP/TAZ phosphorylation in fibroblast of fetal lungs in pseudoglandular stage. FGF10 secreted by mesenchyme, proximal and distal airway markers SOX2 and SOX9 expression decreased branching and caused abnormal branching. Phosphorylation of anti-apoptotic factor SIRT1 after exposure to LPS might be associated with mitigating the injury from inflammation

Supplementary Information

The online version contains supplementary material available at https://doi.org/10.1186/s10020-023-00613-w.

Additional file 1: Figure S1. Representative immunocytochemistry staining of YAP, phosphorylated (p)-YAP, TAZ, and p-TAZ expressions in IMR-90 cells by lipopolysaccharide (LPS) at 0, 10, 30 and 50 μg/mL for 24 h. YAP and TAZ were stained in red, p-YAP and p-TAZ were stained in green, and nuclear staining were marked by DAPI in blue.

Acknowledgements
The authors heartedly thank Ms. Yu-Ling Chung and Yi Syuan Lin for technical assistance during this project.

Author contributions
HCC contributed to the completion of interpretation of the data and completion of the manuscript. HSK and HCC contributed substantially to the concept, the design, interpretation of the data, and completion of the study and the manuscript. HSK and VL contributed to the biochemical analyses. PNT and CMC contributed to critically revising the manuscript for important intellectual content. All authors read and approved the final manuscript.

Funding
This study was funded by the Ministry of Science and Technology of Taiwan (109-2314-B-038-093-MY3).

Availability of data and materials
The datasets used and/or analyzed during the current study are available from the corresponding author on reasonable request.

Declarations

Ethics approval and consent to participate
All animal protocols were prepared in accordance with the Guide for the Care and Use of Laboratory Animals and were approved (IACUC: LAC-2021-0050) by the Laboratory Animal Center at Taipei Medical University (Taipei, Taiwan).

Consent for publication
Not applicable.

Competing interests
The authors declare that they have no conflicts of interest.

Received: 2 August 2022 Accepted: 23 January 2023
Published online: 30 January 2023

References

Alcendor RR, et al. Sirt1 regulates aging and resistance to oxidative stress in the heart. Circ Res. 2007;100:1512–21.

Arai Y, et al. Increased expression of heme oxygenase-1 suppresses airway branching morphogenesis in fetal mouse lungs exposed to inflammation. Pediatr Res. 2020;87:494–500.

Bellusci S, Henderson R, Winnier G, Oikawa T, Hogan BL. Evidence from normal expression and targeted misexpression that bone morphogenetic protein (Bmp-4) plays a role in mouse embryonic lung morphogenesis. Development. 1996;122:1693–702.

Bellusci S, Grindley J, Emoto H, Itoh N, Hogan BL. Fibroblast growth factor 10 (FGF10) and branching morphogenesis in the embryonic mouse lung. Development. 1997;124:4867–78.

Benjamin JT, et al. NF-kappaB activation limits airway branching through inhibition of Sp1-mediated fibroblast growth factor-10 expression. J Immunol. 2010;185:4896–903.

Boström H, et al. PDGF-A signaling is a critical event in lung alveolar myofibroblast development and alveogenesis. Cell. 1996;85:863–73.

Boström H, Gritli-Linde A, Betsholtz C. PDGF-A/PDGF alpha-receptor signaling is required for lung growth and the formation of alveoli but not for early lung branching morphogenesis. Dev Dyn. 2002;223:155–62.

Caniggia I, et al. Spatial and temporal differences in fibroblast behavior in fetal rat lung. Am J Physiol. 1991;261:L424-433.

Caniggia I, Tanswell K, Post M. Temporal and spatial differences in glycosaminoglycan synthesis by fetal lung fibroblasts. Exp Cell Res. 1992;202:252–8.

Cao L, Wang J, Tseu I, Luo D, Post M. Maternal exposure to endotoxin delays alveolarization during postnatal rat lung development. Am J Physiol Lung Cell Mol Physiol. 2009;296:L726-737.

Coughlin MA, et al. Prenatally diagnosed severe CDH: mortality and morbidity remain high. J Pediatr Surg. 2016;51:1091–5.

Dame JB, Juul SE. The distribution of receptors for the pro-inflammatory cytokines interleukin (IL)-6 and IL-8 in the developing human fetus. Early Hum Dev. 2000;58:25–39.

Danopoulos S, et al. Human lung branching morphogenesis is orchestrated by the spatiotemporal distribution of ACTA2, SOX2, and SOX9. Am J Physiol Lung Cell Mol Physiol. 2018;314:L144-l149.

Fernandes-Silva H, et al. Retinoic acid regulates avian lung branching through a molecular network. Cell Mol Life Sci. 2017;74:4599–619.

Fu SL, et al. Hippo signaling pathway in lung development, regeneration, and diseases. Yi Chuan. 2017;39:597–606.

Fu C, et al. Activation of SIRT1 ameliorates LPS-induced lung injury in mice via decreasing endothelial tight junction permeability. Acta Pharmacol Sin. 2019;40:630–41.

Gomez R, et al. The fetal inflammatory response syndrome. Am J Obstet Gynecol. 1998;179:194–202.

Gontan C, et al. Sox2 is important for two crucial processes in lung development: branching morphogenesis and epithelial cell differentiation. Dev Biol. 2008;317:296–309.

Gonzaga S, et al. Cystic adenomatoid malformations are induced by localized FGF10 overexpression in fetal rat lung. Am J Respir Cell Mol Biol. 2008;39:346–55.

Hansen CG, Moroishi T, Guan KL. YAP and TAZ: a nexus for Hippo signaling and beyond. Trends Cell Biol. 2015;25:499–513.

Higgins RD, et al. Evaluation and management of women and newborns with a maternal diagnosis of chorioamnionitis: summary of a workshop. Obstet Gynecol. 2016;127:426–36.

Hogan BL, Yingling JM. Epithelial/mesenchymal interactions and branching morphogenesis of the lung. Curr Opin Genet Dev. 1998;8:481–6.

Hu Y, et al. Activation of MTOR in pulmonary epithelium promotes LPS-induced acute lung injury. Autophagy. 2016;12:2286–99.

Husain AN, Hessel RG. Neonatal pulmonary hypoplasia: an autopsy study of 25 cases. Pediatr Pathol. 1993;13:475–84.

Isago H, et al. Epithelial expression of YAP and TAZ is sequentially required in lung development. Am J Respir Cell Mol Biol. 2020;62:256–66.

Karin M, Ben-Neriah Y. Phosphorylation meets ubiquitination: the control of NF-[kappa]B activity. Annu Rev Immunol. 2000;18:621–63.

Kim CO, Huh AJ, Han SH, Kim JM. Analysis of cellular senescence induced by lipopolysaccharide in pulmonary alveolar epithelial cells. Arch Gerontol Geriatr. 2012;54:e35-41.

Kitada M, Ogura Y, Koya D. The protective role of Sirt1 in vascular tissue: its relationship to vascular aging and atherosclerosis. Aging. 2016;8:2290–307.

Kitaoka H, Burri PH, Weibel ER. Development of the human fetal airway tree: analysis of the numerical density of airway endtips. Anat Rec. 1996;244:207–13.

Kunzmann S, Collins JJ, Kuypers E, Kramer BW. Thrown off balance: the effect of antenatal inflammation on the developing lung and immune system. Am J Obstet Gynecol. 2013;208:429–37.

LaCanna R, et al. Yap/Taz regulate alveolar regeneration and resolution of lung inflammation. J Clin Invest. 2019;129:2107–22.

Land SC, Darakhshan F. Thymulin evokes IL-6-C/EBPbeta regenerative repair and TNF-alpha silencing during endotoxin exposure in fetal lung explants. Am J Physiol Lung Cell Mol Physiol. 2004;286:L473-487.

Lawrence T. The nuclear factor NF-kappaB pathway in inflammation. Cold Spring Harb Perspect Biol. 2009;1: a001651.

Lin C, Yao E, Chuang P-T. A conserved MST1/2–YAP axis mediates Hippo signaling during lung growth. Dev Biol. 2015;403:101–13.

Lin C, et al. YAP is essential for mechanical force production and epithelial cell proliferation during lung branching morphogenesis. Elife. 2017;6: e21130.

Liu LY, et al. YAP activity protects against endotoxemic acute lung injury by activating multiple mechanisms. Int J Mol Med. 2020;46:2235–50.

Long Y, et al. Oxidative stress and NF-κB signaling are involved in LPS induced pulmonary dysplasia in chick embryos. Cell Cycle. 2018;17:1757–71.

Luo J, et al. Negative control of p53 by Sir2alpha promotes cell survival under stress. Cell. 2001;107:137–48.

Mahoney JE, Mori M, Szymaniak AD, Varelas X, Cardoso WV. The hippo pathway effector Yap controls patterning and differentiation of airway epithelial progenitors. Dev Cell. 2014;30:137–50.

Makita R, et al. Multiple renal cysts, urinary concentration defects, and pulmonary emphysematous changes in mice lacking TAZ. Am J Physiol Renal Physiol. 2008;294:F542-553.

Massagué J, Chen YG. Controlling TGF-beta signaling. Genes Dev. 2000;14:627–44.

Mia MM, Singh MK. Emerging roles of the Hippo signaling pathway in modulating immune response and inflammation-driven tissue repair and remodeling. FEBS J. 2022;289:4061–81.

Mitani A, et al. Transcriptional coactivator with PDZ-binding motif is essential for normal alveolarization in mice. Am J Respir Crit Care Med. 2009;180:326–38.

Monteiro JP, Cano MI. SIRT1 deacetylase activity and the maintenance of protein homeostasis in response to stress: an overview. Protein Pept Lett. 2011;18:167–73.

Muraoka RS, Bushdid PB, Brantley DM, Yull FE, Kerr LD. Mesenchymal expression of nuclear factor-kappaB inhibits epithelial growth and branching in the embryonic chick lung. Dev Biol. 2000;225:322–38.

Muratore CS, et al. Endotoxin alters early fetal lung morphogenesis. J Surg Res. 2009;155:225–30.

Murthy V, Kennea NL. Antenatal infection/inflammation and fetal tissue injury. Best Pract Res Clin Obstet Gynaecol. 2007;21:479–89.

Nantie LB, et al. Lats1/2 inactivation reveals Hippo function in alveolar type I cell differentiation during lung transition to air breathing. Development. 2018;145: dev163105.

Nogueira-Silva C, Santos M, Baptista MJ, Moura RS, Correia-Pinto J. IL-6 is constitutively expressed during lung morphogenesis and enhances fetal lung explant branching. Pediatr Res. 2006;60:530–6.

Pocaterra A, Romani P, Dupont S. YAP/TAZ functions and their regulation at a glance. J Cell Sci. 2020;133: jcs230425.

Rehan VK, Wang Y, Patel S, Santos J, Torday JS. Rosiglitazone, a peroxisome proliferator-activated receptor-gamma agonist, prevents hyperoxia-induced neonatal rat lung injury in vivo. Pediatr Pulmonol. 2006;41:558–69.

Rockich BE, et al. Sox9 plays multiple roles in the lung epithelium during branching morphogenesis. Proc Natl Acad Sci USA. 2013;110:E4456-4464.

Sarno L, et al. Histological chorioamnionitis and risk of pulmonary complications in preterm births: a systematic review and meta-analysis. J Matern Fetal Neonatal Med. 2021;34:3803–12.

Sasaki T, et al. Phosphorylation regulates SIRT1 function. PLoS ONE. 2008;3: e4020.

Sekine K, et al. Fgf10 is essential for limb and lung formation. Nat Genet. 1999;21:138–41.

Shihan MH, Novo SG, Le Marchand SJ, Wang Y, Duncan MK. A simple method for quantitating confocal fluorescent images. Biochem Biophys Rep. 2021;25: 100916.

Smith LJ, McKay KO, van Asperen PP, Selvadurai H, Fitzgerald DA. Normal development of the lung and premature birth. Paediatr Respir Rev. 2010;11:135–42.
Tita AT, Andrews WW. Diagnosis and management of clinical chorioamnionitis. Clin Perinatol. 2010;37:339–54.
Tompkins DH, et al. Sox2 activates cell proliferation and differentiation in the respiratory epithelium. Am J Respir Cell Mol Biol. 2011;45:101–10.
Torday JS, Rehan VK. On the evolution of the pulmonary alveolar lipofibroblast. Exp Cell Res. 2016;340:215–9.
Tsuda A, et al. The relationship between amniotic fluid interleukin-6 concentration and histologic evidence of chorioamnionitis. Acta Obstet Gynecol Scand. 1998;77:515–20.
Ushakumary MG, Riccetti M, Perl AT. Resident interstitial lung fibroblasts and their role in alveolar stem cell niche development, homeostasis, injury, and regeneration. Stem Cells Transl Med. 2021;10:1021–32.
Volckaert T, et al. Hippo signaling promotes lung epithelial lineage commitment by curbing Fgf10 and β-catenin signaling. Development. 2019;146: dev166454.
Wang Y, Yu A, Yu F-X. The Hippo pathway in tissue homeostasis and regeneration. Protein Cell. 2017;8:349–59.
Wang J, Liu H, Gao L, Liu X. Impaired FGF10 signaling and epithelial development in experimental lung hypoplasia with esophageal atresia. Front Pediatr. 2018a;6:109.
Wang W, et al. JAK1-mediated Sirt1 phosphorylation functions as a negative feedback of the JAK1-STAT3 pathway. J Biol Chem. 2018b;293:11067–75.
Wang R, Xie Y, Qiu J, Chen J. The effects of dexmedetomidine in a rat model of sepsis-induced lung injury are mediated through the adenosine monophosphate-activated protein kinase (AMPK)/silent information regulator 1 (SIRT1) pathway. Med Sci Monit. 2020;26: e919213.
Warburton D, et al. Growth factor signaling in lung morphogenetic centers: automaticity, stereotypy and symmetry. Respir Res. 2003;4:5.
Wessells NK. Mammalian lung development: interactions in formation and morphogenesis of tracheal buds. J Exp Zool. 1970;175:455–66.
Yin Y, Ornitz DM. FGF9 and FGF10 activate distinct signaling pathways to direct lung epithelial specification and branching. Sci Signal. 2020;13: eaay4353.
Zepp JA, et al. Distinct mesenchymal lineages and niches promote epithelial self-renewal and myofibrogenesis in the lung. Cell. 2017;170:1134-1148. e1110.
Zhao J, Lee M, Smith S, Warburton D. Abrogation of Smad3 and Smad2 or of Smad4 gene expression positively regulates murine embryonic lung branching morphogenesis in culture. Dev Biol. 1998;194:182–95.

Publisher's Note

Springer Nature remains neutral with regard to jurisdictional claims in published maps and institutional affiliations.

Ready to submit your research? Choose BMC and benefit from:

- fast, convenient online submission
- thorough peer review by experienced researchers in your field
- rapid publication on acceptance
- support for research data, including large and complex data types
- gold Open Access which fosters wider collaboration and increased citations
- maximum visibility for your research: over 100M website views per year

At BMC, research is always in progress.

Learn more biomedcentral.com/submissions

BMC